Nov 16th, 12:00 AM

The Strength of Cold-formed Portal Frames

A. H. Baigent

Gregory J. Hancock

THE STRENGTH OF COLD-FORMED PORTAL FRAMES

by

A.H. Baigent *

and

G.J. Hancock **

Summary

The collapse behaviour of seven pitched roof portal frames constructed by bolting cold-formed channels together using stiffened plates is described. Analytical methods which determine progressive yielding and inelastic local buckling in thin-walled channel sections are described. The theoretical structural response is compared with the portal frame tests.

* Victorian Manager, Longworth and McKenzie Pty Limited, Melbourne, Victoria, Australia.

** Senior Lecturer, School of Civil and Mining Engineering, University of Sydney, NSW, Australia.

1. INTRODUCTION

For over 20 years, the use of cold-formed members has been common for secondary structural systems such as the purlins and girts used in industrial buildings. However the use of cold-formed members for the primary structural system such as the main portal frames has been comparatively rare. The recent availability of larger cold-formed sections and efficient jointing systems for cold-formed members has allowed economic industrial buildings composed entirely of cold-formed members to be produced.

The designer of such a structure requires a knowledge of both the stiffness and strength of the structural system. A method of structural analysis using the matrix displacement method for the linear elastic response of structures composed of thin-walled members was described briefly by the authors in Ref. 3, and in more detail in Ref. 4. The method allows the deflections and the stress resultants at critical cross-sections to be determined. If a design based on first yield is to be produced, this linear analysis would be sufficient.

After initial localised yielding, the structure may carry a substantial increase in load before failure. In the design of portal frames composed of hot-rolled members with stocky plate elements, plastic hinges (Ref. 1) are permitted at points around the frame. Recent amendments to the AISI spec. (Section 3.9, Ref. 2) have permitted plasticity in cold-formed members with low plate slenderness ratios (compact sections).

However, structures with more slender plate elements may also support a substantial load after yielding before collapse. In this case, a combined failure mode involving yielding and local buckling at critical cross-sections will occur.

In this paper, the behaviour of structures in this latter category is described. Firstly the configuration and results of the frame tests are presented. Then the analytical techniques used to predict the frame yield and collapse loads are developed. The analytical methods involve three stages which are:-

(a) Calculation of the stress-resultants at critical cross-sections in a thin-walled structure.

(b) Calculation of progressive yielding at critical cross-sections.

(c) Determination of the ultimate strength of the structure based on inelastic local buckling at critical cross-sections.

2. FRAME TESTS

An experimental study of seven pinned-base pitched-roof portal frames with the geometry shown in Figure 1 was described by the authors in Ref. 3. These frames consisted of cold formed channels bent about their major axes and bolted together through their webs using joints of the type shown in Figure 2. The channel used in the study had an overall depth of 153mm (6 in.), an overall width of 79mm (3.11 in.), a plate thickness of 1.86mm (0.073 in.), an overall lip stiffener depth of 15mm (0.59 in.) and internal corner radii of 10mm (0.39 in.).

Lateral restraint consisted of two types. External restraint simulated the effect of purlins and girts and involved prevention of movement normal to the plane of the frame at the sixteen locations shown in Figure 1. External and internal restraint simulated the effect of purlins and girts with fly bracing and involved prevention of lateral movement of the internal flange of the frame as well as the external restraint described above. The internal lateral restraints were located opposite the third external restraint position in each stanchion and opposite the first and third restraint positions in each rafter.

The three different load sets used in the study are shown in Figure 3. The loads were applied to the frame at the restraint points since the lateral restraints in the experimental study had assumed the function of purlins and girts. The restraint and loading configurations used in the seven tests are summarised in Table 1.

The experimental first yield and collapse loads are set out for each of the seven frames in Table 1. The first yield loads were determined from strain gauges located around the section at critical cross-sections of the frames. The detail of the positions of these gauges are given in Section 3.2.

Tension specimens were taken from the flat portions of the cold-formed channel sections of each frame where cold-working had not altered the stress-strain curve of the virgin material. A total of 84 specimens were tested and the mean static yield stress was 325.8 MPa (47.3 ksi). The static yield stress was used in all calculations since it is regarded as the yield stress which would be maintained by a yielding section of the frame under static gravity loading after the upper yield point had been reached. The experimental first yield loads were determined when the measured strain readings of any strain gauge reached or exceeded a value of 1590 microstrain.

3. CALCULATION OF THE STRESS DISTRIBUTION IN A THIN-WALLED STRUCTURE

3.1 Method

The matrix displacement analysis of thin-walled structures described in Ref. 4 is based on a conventional space frame analysis but includes the effects of cross-section asymmetry or monosymmetry, non-uniform torsion, eccentric restraints as well as joint types peculiar to thin-walled members. On completion of the analysis, the stress resultants at the end of each element are calculated. These stress

resultants include those shown in Figure 4 which produce longitudinal stress. These are the axial force (F_z), the bending moments about the x, y axes (M_x, M_y) and the bimoment (B_z) (Ref. 19) resulting from non-uniform torsion or from bending moment applied in a plane of the thin-walled section eccentric from the shear centre. In the case of the test portal frames, a bimoment is applied on the end of each member as a result of the major axis moment which is located in the plane of the web and eccentric from the shear centre of the channel.

3.2 Comparison with Experiment

For each of the seven frames tested, the calculated stress distributions at critical cross-sections showed that the section immediately below the eaves would yield first. Hence the eleven strain gauges (3 on each flange and 5 on the web) were located on the cross-sections as shown in Figures 5 and 6 at a position 25mm (1.0 in.) below the eaves joint. The resulting measured longitudinal stress distributions have been compared in Figures 5 and 6 with those calculated theoretically.

The stress distributions are principally a combination of major axis moment and bimoment with a resulting non-uniform stress distribution across the flanges. The most highly stressed point occurs at the flange web junction. In all cases, the theoretical and experimentally measured stress distributions are in fairly close agreement.

4. CALCULATION OF PROGRESSIVE YIELDING IN THIN-WALLED CROSS-SECTIONS

4.1 Method

Following initial yielding at a cross-section, increasing load causes yielding to progress along the thin-walled elements of the cross-

section. In the case of the sections shown in Figures 5 and 6, yielding commences at the flange-web junction and penetrates into both the web and flange. To calculate the progression of yielding, it is assumed that the stress resultant ratios calculated at first yield remain constant so that a monotonic load increase can be applied. This assumption is reasonable for small increases in load beyond first yield where the localised yielding does not alter significantly the overall structural response. However, where yielding produces significant areas of plasticity, this assumption will generally produce conservative results since the yielded zones calculated will be greater than in reality.

Santathadaporn and Chen (Ref. 16) developed a tangent stiffness method for the biaxial bending analysis of column sections. However their method did not include yielding resulting from warping torsion of thin-walled members. The second author extended the method described in Ref. 16 to include yielding resulting from bimoment and applied the method in Ref. 10 to study I-sections yielding as a result of warping torsion as well as biaxial bending. The first author developed the method for thin-walled sections of any general geometry and applied it to a study of channel sections in Ref. 6. A brief summary of the principles involved in the method follows and a detailed mathematical description is given in Ref. 5.

Firstly, the axial force, bending moments and bimoment shown in Figure 4 are increased monotonically beyond yield by applying a load factor (λ) to their values. Based on the elastic section rigidities (EA, EI_x, EI_y, EI_w), the resulting strain distribution is calculated. The yielded zones are determined and the consequent stress distribution assuming the yield stress in yielded zones is integrated to calculate the nett section stress resultants. Before convergence, these stress resultants will differ slightly from the applied values at load factor (λ). The axial strain (ε_z), curvatures (ρ_x, ρ_z) and rate of change of twist (ϕ''_z) are adjusted using a tangent stiffness matrix based on

the effective section rigidities. The effective rigidities are those of the elastic core ignoring yielded zones. A new strain distribution and hence yield distribution is calculated and the process repeated until convergence. At this stage, the resulting stress distribution including yielded zones is in equilibrium with the applied stress resultants. By continuing this process at increasing load factor (λ), the progression of yielding in a thin-walled cross-section can be calculated.

4.2 Comparison with Experiment

The progression of yielding at the cross-sections for which the stress distributions have been plotted in Figures 5 and 6 were determined from the measured strain distributions at increasing load levels. The analytical method described in Section 4.1 was used to compute the progression of yielding for comparison with the test results. Two basic types of behaviour occurred and typical results for frames 5 and 6 representing these two types are presented in Figures 7 and 8 respectively.

The theoretical results for frame 5 in Figure 7 (b) show a similar response to the experimental values in Figure 7 (a). This level of agreement is similar for all frames up to 1.20 times the first yield load. At an experimental load factor of 1.32 times the experimentally measured first yield load, inelastic local buckling occurred at the critical cross-section and the frame collapsed. The theoretically computed collapse load determined by the method described in the next section (5.1) was 1.28 times the theoretical first yield load.

The theoretical results for frame 6 in Figure 8 (b) show a similar response up to approximately 1.25 times the first yield load. However, after that point the experimentally measured rate of progression of yielding dropped significantly and collapse occurred at a load factor of 1.54 times the experimentally measured first yield. By comparison, the theoretically computed progression of yield does not

exhibit such behaviour and theoretical collapse would occur at 1.17 times the theoretical first yield load. Strain-hardening, which is not accounted for in the analysis, appears to have restricted the rate of progression of yield in this case.

Frames 2, 3 exhibited behaviour similar to frame 5 and frames 4, 7 exhibited behaviour similar to frame 6.

5. CALCULATION OF STRUCTURAL STRENGTH

5.1 Method

As described in the previous section, failure of the frames occurred when inelastic local buckles developed at critical cross-sections. To calculate theoretically the inelastic buckling load, a method is required which accounts for the particular geometry of the cross-section, the longitudinal stress distribution and the progression of yielding. Yoshida (Ref. 18) described a method in which he used the finite strip method of analysis developed by Y.K. Cheung (Ref. 8) and which was applied to local buckling by Przemieniecki (Ref. 15). Yoshida extended the elastic analysis in Ref. 15 by allowing for yielding in I-section columns. He achieved this by reducing the effective moduli of yielded strips according to the theory of plastic stability of thin-walled plates described by Bijlaard (Ref. 7).

In this paper, a similar method is applied to channel sections. A finite strip subdivision of the channel is shown in Figure 9. The detailed analytical method of elastic buckling analysis was described by the second author in Ref. 11. The method involves performing a buckling analysis of the section subjected to the appropriate longitudinal stress distribution for an assumed range of buckle half-wavelengths. The resulting critical stresses for local buckling are plotted against the buckle half-wavelengths as shown in Figure 10. The modes corresponding to certain half-wavelengths are

shown in Figure 11. The mode shown in Figure 11 (a) is a local buckle involving the flange and web and occurs at the minimum shown in Figure 10 at L = 90 mm (3.5 in.). Another higher minimum occuring at L = 550 mm (21.6 in.) and corresponding to a stiffener buckle is shown in Figure 11 (b). For long wavelengths of laterally unrestrained sections, a lateral buckle of the type shown in Figure 11 (c) occurs. However for the test frames, lateral restraints prevented this mode and so the local mode shown in Figure 11 (a) would predominate.

To account for yielding, the analytical process is performed with the Youngs and Shear moduli and Poisson's ratio of yielded strips reduced to allow for plasticity. A rational theory of inelastic local buckling was developed by Ilyushin (Ref. 12) and Stowell (Ref. 17). Stowell concluded that the tangent modulus should be used in the longitudinal direction and the elastic modulus transversely. However Popov and Medwadowski (Ref. 14) have concluded that the use of the tangent modulus in both directions produces sufficiently accurate results. Accordingly, in this paper a value of E/E_t equal to 33 in both directions has been chosen.

The inelastic shear modulus is also open to conjecture. Haaijer (Ref. 9) and Lay (Ref. 13) have concluded that a shear modulus based on mild steel under torsion in the strain-hardening range produces reasonable results. Accordingly, in this paper, G_y/G has been taken as 0.25 based on the work of Lay. Poisson's ratio has been assumed to be 0.3 in the elastic region and 0.5 for the inelastic material.

The results of the inelastic local buckling analysis at increasing load factors are shown in Figure 12. The buckling curves are seen to drop with increasing load factor without a significant change in the buckle half-wavelength. When the minimum on the buckling curve is equal to the load factor, failure is assumed to occur.

5.2 Comparison with Experiment

The theoretical collapse and first yield loads calculated by the method described above have been included in Table I. For frames 2, 3 and 5 which developed inelastic local buckles below the eaves before strain-hardening, the ratio of the experimental to theoretical collapse loads are 1.07, 1.10 and 1.01 respectively. However for frames 4, 6 and 7 for which strain-hardening arrested yielding before inelastic local buckling could occur, the corresponding ratios are 1.45, 1.27 and 1.45 respectively. In these latter cases, collapse of the frame occurred when local buckling also took place within the rafters.

The method developed appears to provide an accurate estimate of collapse if inelastic local buckling occurs before strain-hardening influences take effect. However if strain-hardening prevents inelastic local buckling, the frames may carry a substantial increase in load.

In all cases, the analytical method provided a lower bound to collapse. The computed ratios of collapse to first yield were 1.17, 1.24, 1.21, 1.28, 1.17, 1.22. Hence a theoretical overload capacity ranging from 17 to 28 percent of first yield is permissible. This is to be expected in a situation where longitudinal stresses resulting from bimoment form a significant part of the total stress causing yield.

6. CONCLUSIONS

Measurements of stress at critical cross-sections of portal frames composed of cold formed members indicate that theoretical stress estimates soundly based on thin-walled theory produce accurate predictions. Calculations of progressive yielding after first yield are also fairly accurate provided that strain hardening does not arrest the yielding pattern.

For the portal frames tested for which the theoretical elastic local buckling loads were two to three times the first yield load, the structures were able to support loads significantly higher than those which would cause first yield. The increased load capacity was partly a result of the stress distribution produced by combined major axis moment and warping torsion (bimoment). This stress distribution caused progressive yielding of the flange of the channel section unlike the case of pure major axis moment which would cause the full width of compression flange to yield simultaneously.

Theoretical estimates of the inelastic local buckling load at critical cross-sections were accurate provided that strain-hardening did not arrest yielding. In this latter case, inelastic local buckling was delayed and loads substantially in excess of first yield could be supported by the frames.

7. ACKNOWLEDGEMENTS

The work has been carried out in the School of Civil and Mining Engineering at the University of Sydney. Calculations were performed in the C.A. Hawkins Computing Laboratory at a terminal to a PRIME minicomputer. Funds to purchase this system were provided by members of the Civil Engineering Graduates Association. The tests were performed in the J.W. Roderick Structures Laboratory at the University of Sydney.

Support for this work was given by a grant from the Australian Research Grants Committee. The first author was supported by a Commonwealth Post-graduate Research Award.

8. APPENDIX - REFERENCES

1. American Institute of Steel Construction, Specification for the Design, Fabrication and Erection of Structural Steel for Buildings, Part 2, February 1969.

2. American Iron and Steel Institute, Specification for the Design of Cold-Formed Steel Structural Members, Washington, D. C., September, 1980.

3. Baigent, A.H. and Hancock, G.J., The Behaviour of Portal Frames Composed of Cold-Formed Members, Proceedings, International Conference on Thin-Walled Structures, University of Strathclyde, April, 1979.

4. Baigent, A.H. and Hancock, G.J., Structural Analysis of Assemblages of Thin-Walled Members, Research Report, The University of Sydney, School of Civil Engineering, R389, June 1981, (accepted for publication in 'Engineering Structures' in 1982).

5. Baigent, A.H. and Hancock, G.J., The Strength of Portal Frames Composed of Cold-Formed Channels, Research Report, The University of Sydney, School of Civil and Mining Engineering, R407, March 1982.

6. Baigent, A.H., Thin-Walled Structural Systems, Ph.D. Thesis, University of Sydney, June 1980.

7. Bijlaard, P.P., Theory of Plastic Stability of Thin Plates, Publications, IABSE, Zurich, Vol. 6 1940.

8. Cheung, Y.K., Finite Strip Method in Structural Analysis, Pergamon Press, Inc., New York, NY, 1976.

9. Haaijer, G., Plate Buckling in the Strain Hardening Range, Journal of the Engineering Mechanics Division, ASCE, Vol. 83, No. EM2, April 1957.

10. Hancock, G.J., Elastic - Plastic Analysis of Thin-Walled Cross-Sections, Proceedings, 6th Australasian Conference on the Mechanics of Structures and Materials, Christchurch, New Zealand, August, 1977.

11. Hancock, G.J., Local, Distortional and Lateral Buckling of I-Beams, Journal of the Structural Division, ASCE, Vol. 104, No. ST11, November, 1978.

12. Ilyushin, A.A., The Elasto-Plastic Stability of Plates, NACA Technical Memorandum, TM 1188, 1947 (translation from Russian).

13. Lay, M.G., Flange Local Buckling in Wide Flange Shapes, Journal of the Structural Division, ASCE, Vol. 91, No. ST6, December 1964.

14. Popov, E.P., and Medwadowski, S.J., Stability of Reinforced Concrete Shells, State of the Art Overview, Draft Report.

15. Przemieniecki, J.S., Finite Element Structural Analysis of Local Instability, Journal of the American Institute of Aeronautics and Astronautics, Vol. 11, No. 1, January, 1973.

16. Santathadaporn, S., and Chen, W.F., Tangent Stiffness Method for Biaxial Bending, Journal of the Structural Division, Proceedings, ASCE, Vol. 98, No. ST1, January, 1972.

17. Stowell, E.A., A Unified Theory of Plastic Buckling of Columns and Plates, NACA Technical Note, TN 1556, 1948.

18. Yoshida, H., Coupled Strength of Local and Whole Bucklings of H Columns, Proceedings of the Japan Society of Civil Engineers, No. 243, November, 1975 (In Japanese).

19. Vlasov, V.Z., Thin-Walled Elastic Beams, Moscow, 1959, (English Translation, Israel Program for Scientific Translations, Jerusalem, 1961).

FRAME NO	RESTRAINT	LOAD CASE	EXPERIMENTAL COLLAPSE LOAD kN	EXPERIMENTAL YIELD LOAD kN	THEORETICAL COLLAPSE LOAD kN	THEORETICAL YIELD LOAD kN
1	External	1	16.40	-	15.37	13.1
2	External	1	16.40	11.5	15.37	13.1
3	External	2	20.44	15.7	18.62	15.0
4	External	3	37.81	21.4	26.04	21.5
5	External & Internal	1	18.40	13.9	18.30	14.3
6	External & Internal	2	24.44	15.9	19.29	16.5
7	External & Internal	3	40.15	22.8	27.62	22.6

(1 KIP = 4.445 kN)

TABLE 1 - FRAME COLLAPSE AND YIELD LOADS

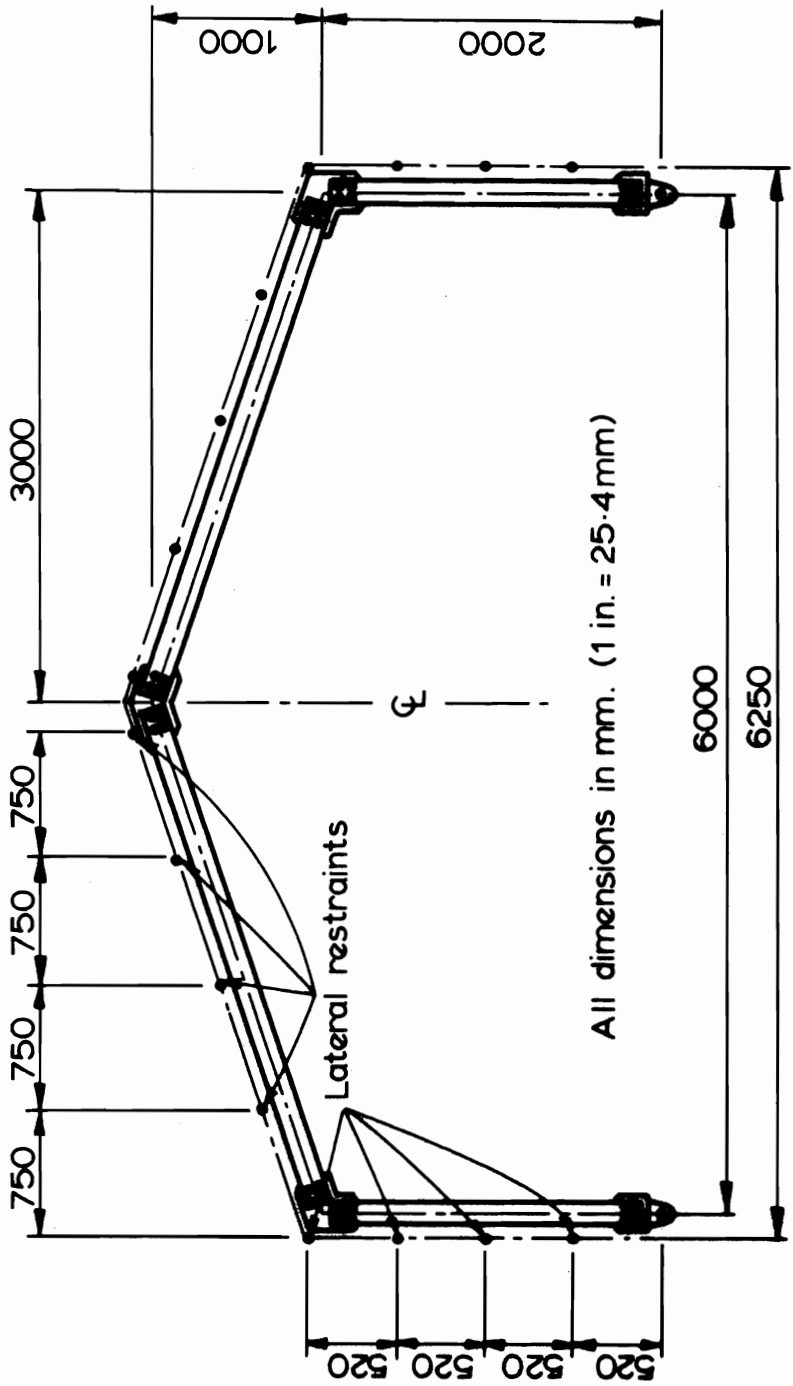

FIG. 1 FRAME GEOMETRY

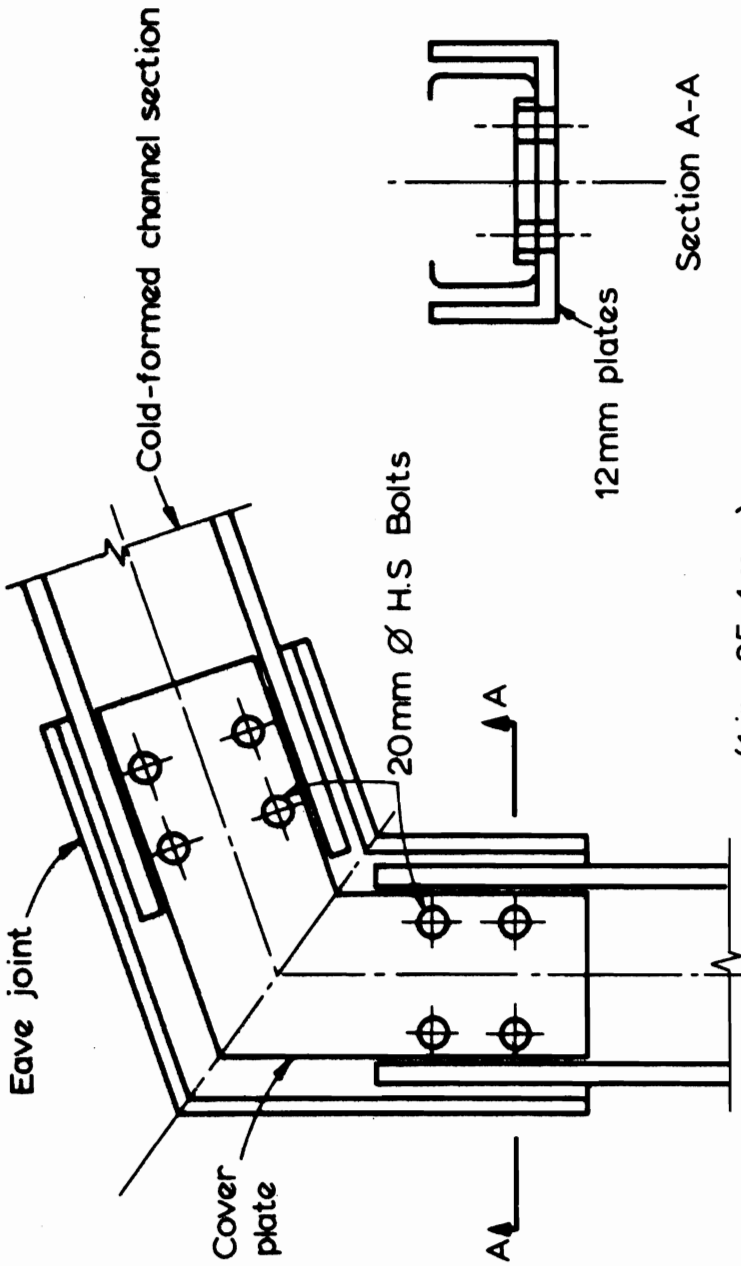

FIG.2 JOINT DETAILS

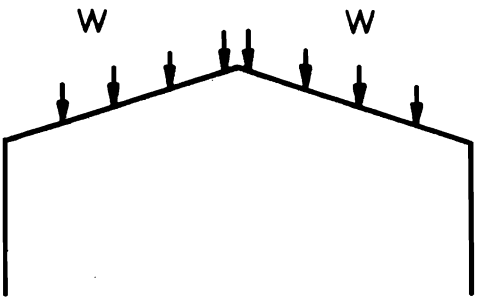

(a) Load case 1
Dead load and
live load

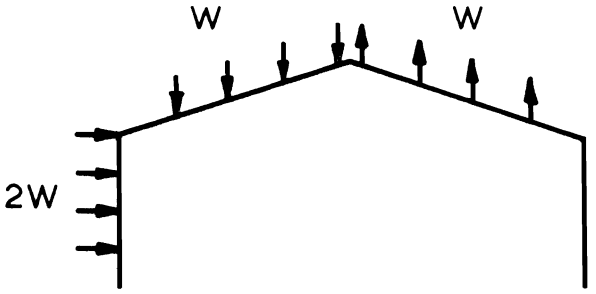

(b) Load case 2
Transverse
wind load

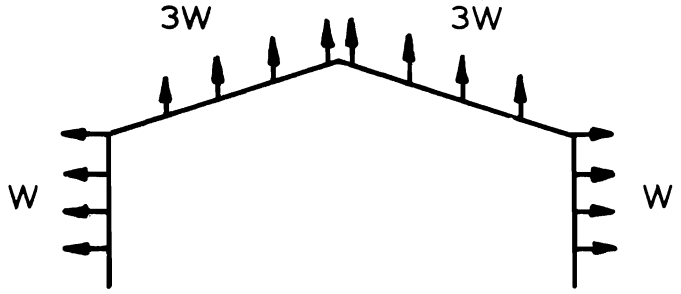

(c) Load case 3
Longitudinal
wind load

FIG. 3 LOADING PATTERNS

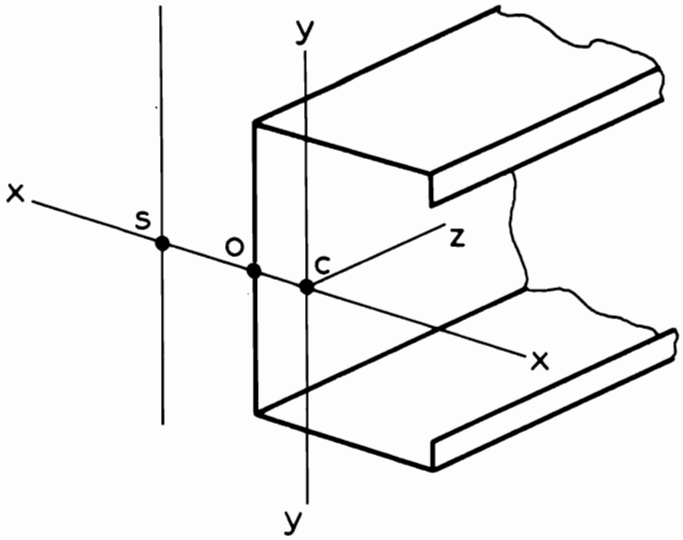

(i)

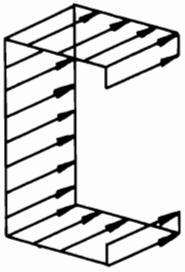

(ii) F_z

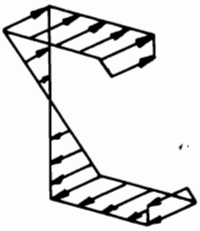

(iii) M_x

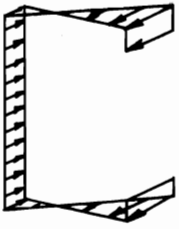

(iv) M_y

(v) B_z

FIG. 4 STRESSES IN A CHANNEL SECTION

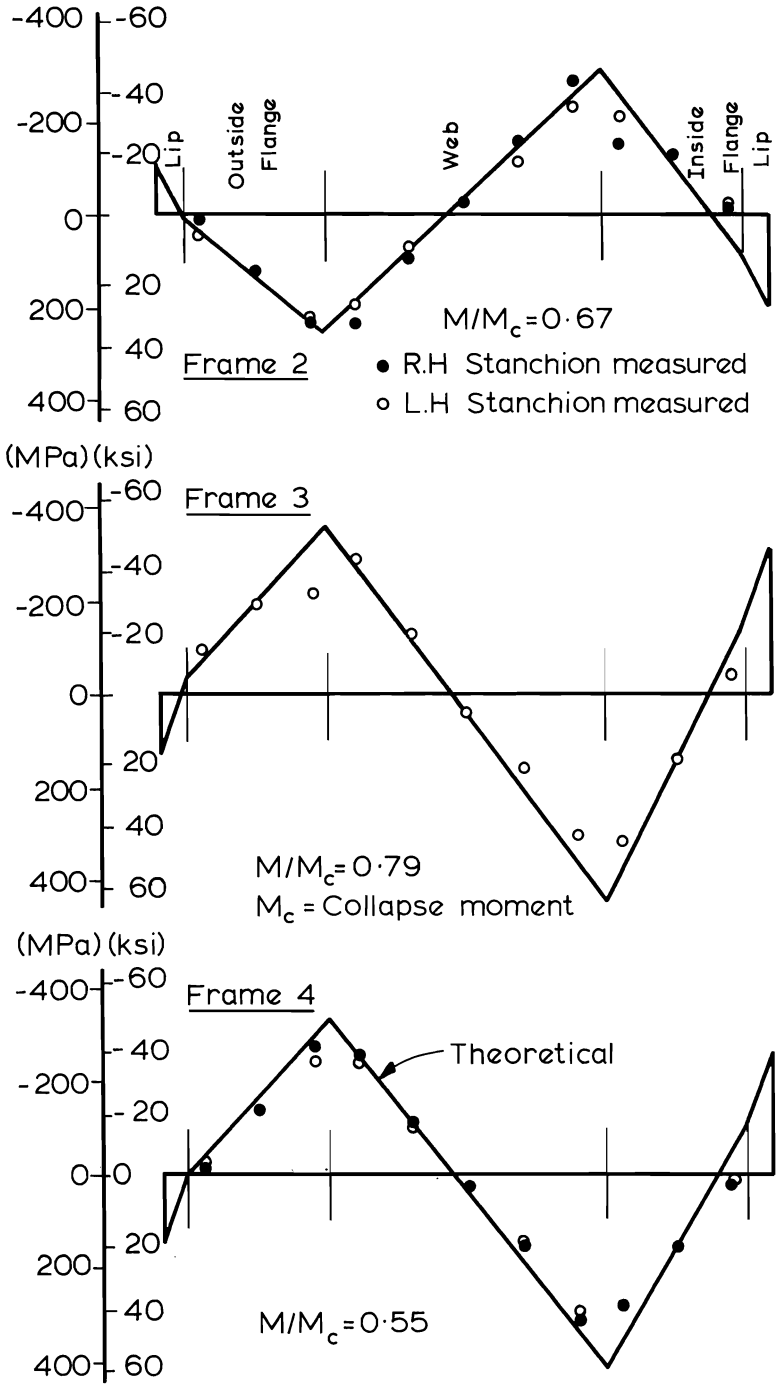

FIG. 5 STRESS DISTRIBUTIONS BELOW EAVES (FRAMES 2,3,4)

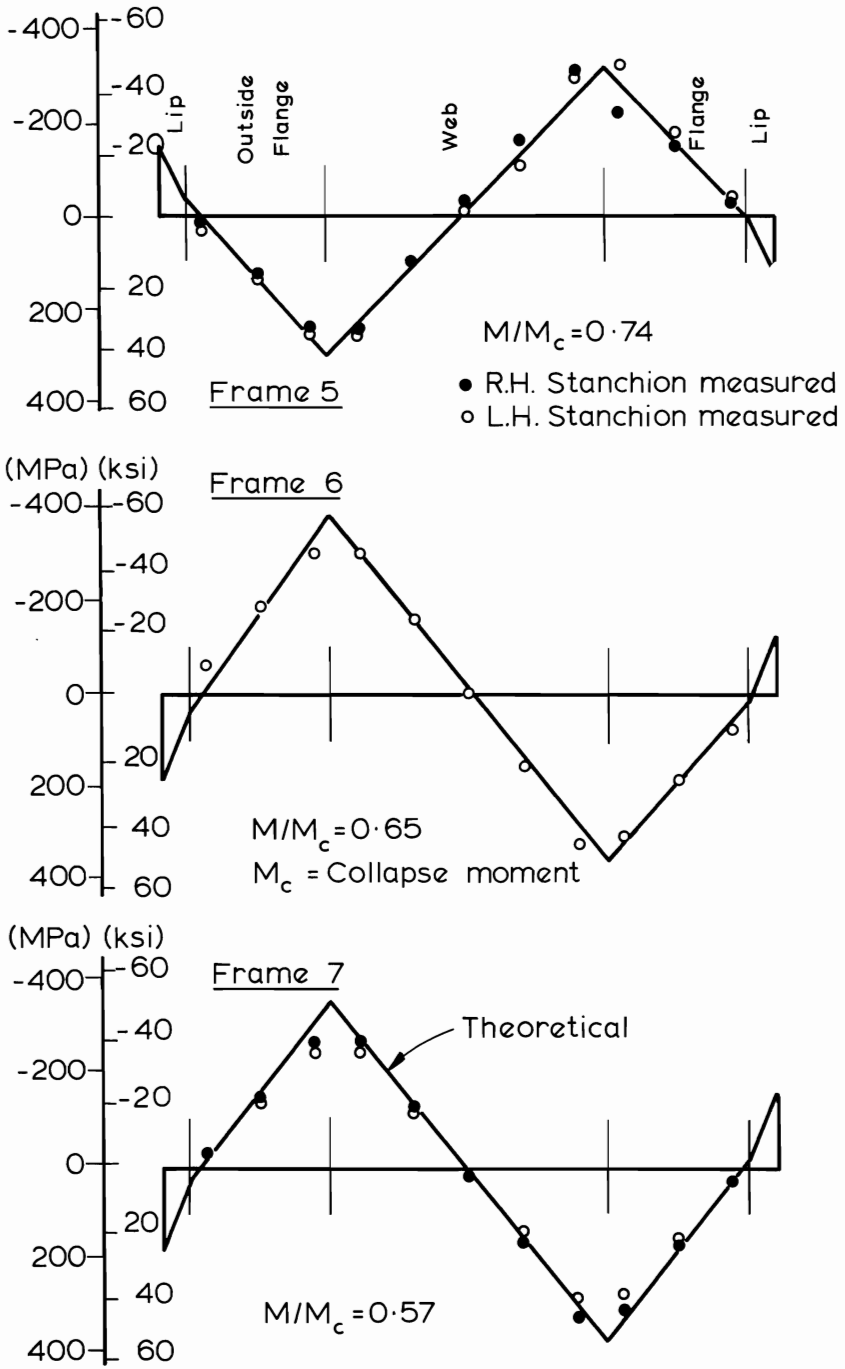

FIG. 6 STRESS DISTRIBUTIONS BELOW EAVES (FRAMES 5,6,7)

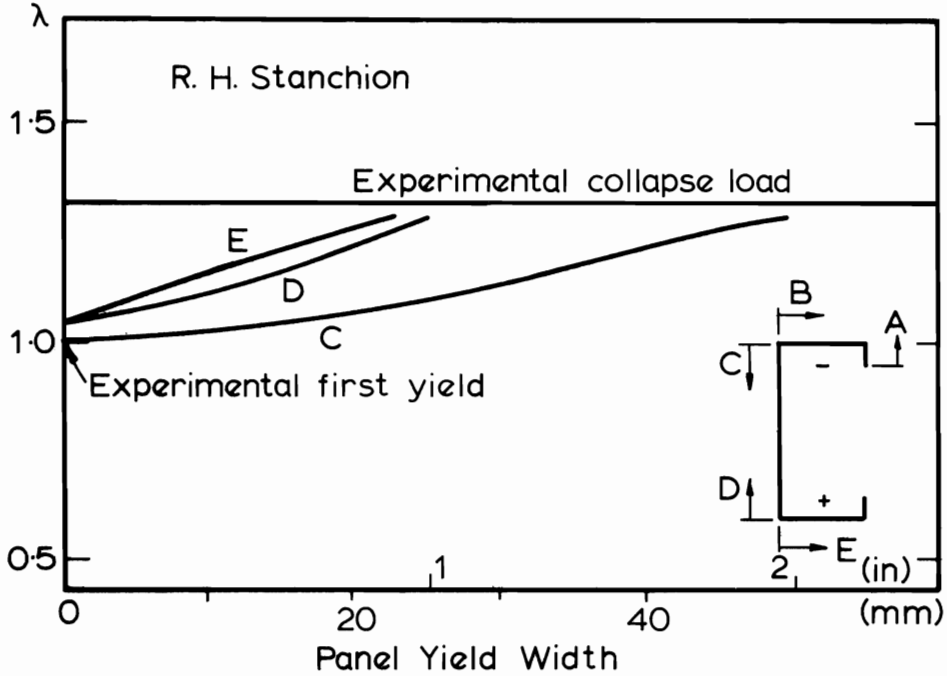

(a) Experimental

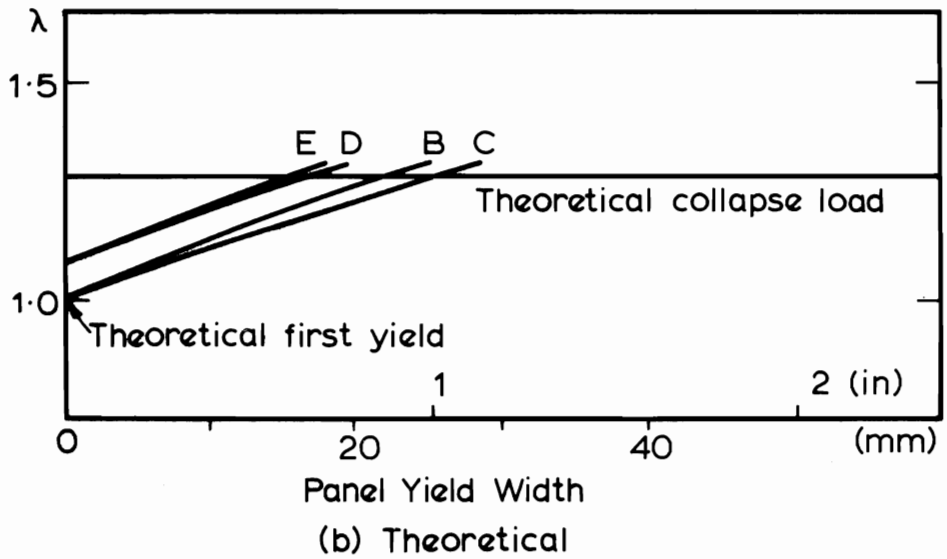

(b) Theoretical

FIG. 7 COMPARISON OF PANEL YIELDING FOR FRAME 5

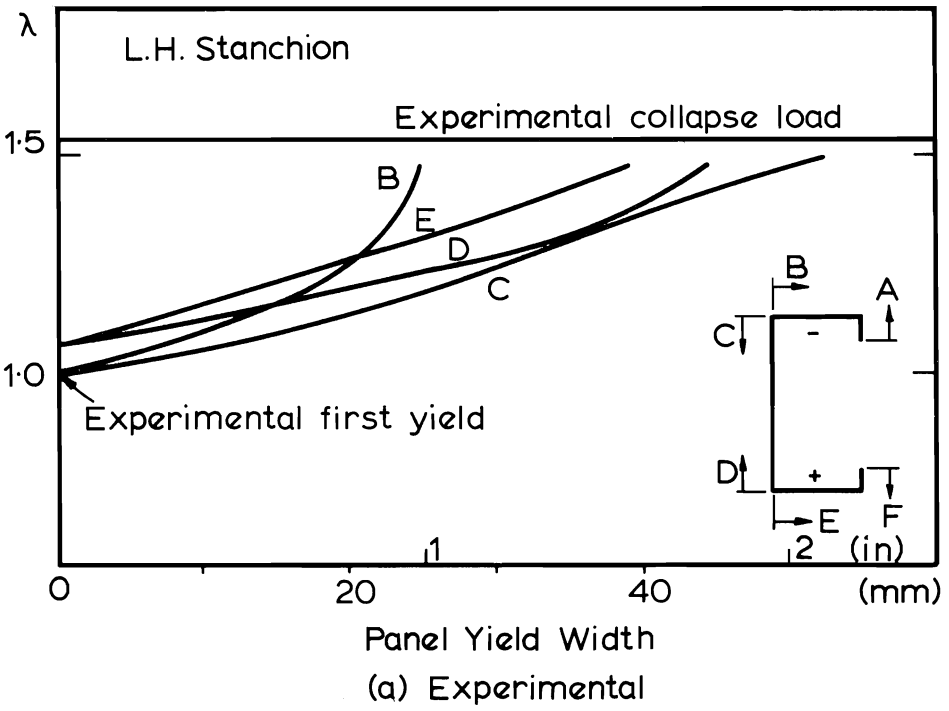

(a) Experimental

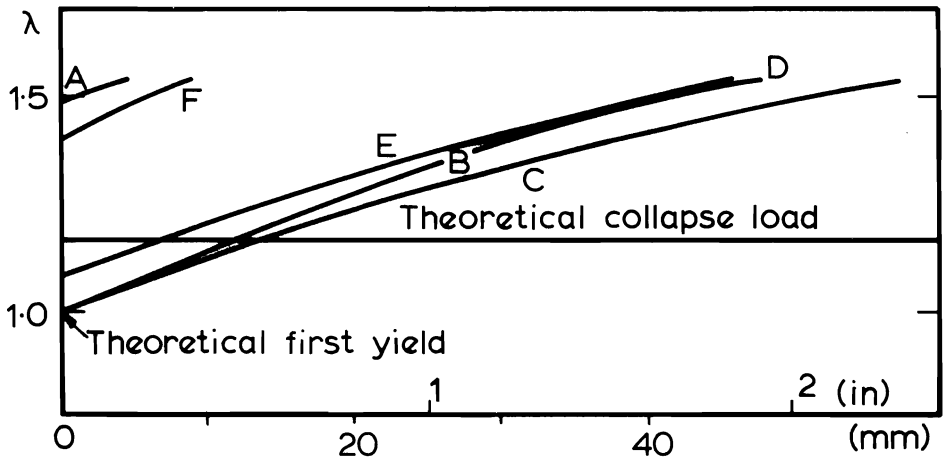

(b) Theoretical

FIG. 8 COMPARISON OF PANEL YIELDING FOR FRAME 6

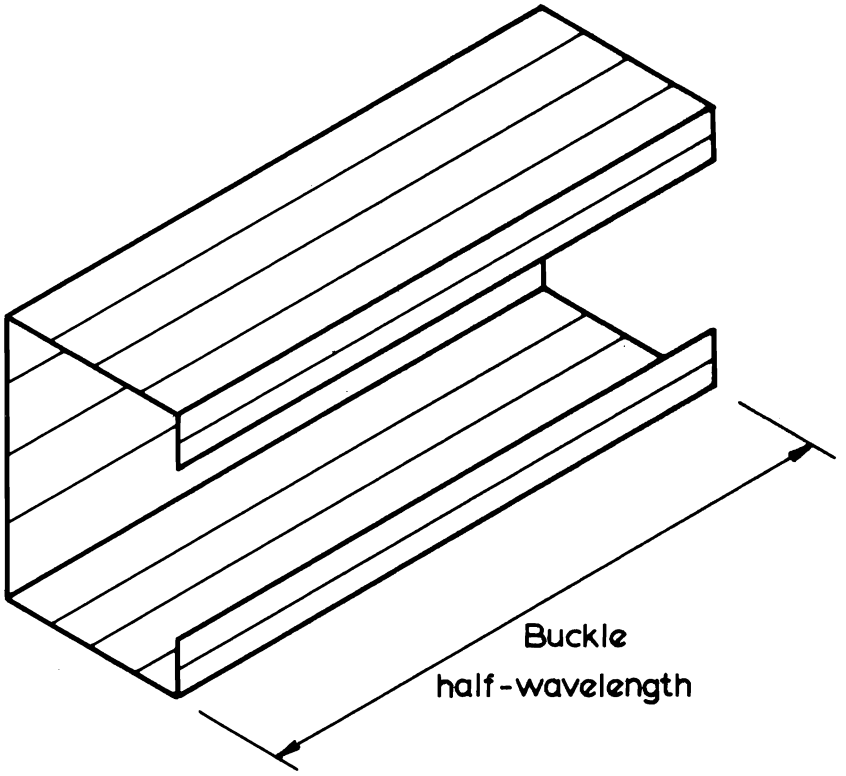

FIG. 9 FINITE STRIP SUBDIVISION OF CHANNEL SECTION FOR BUCKLING ANALYSIS

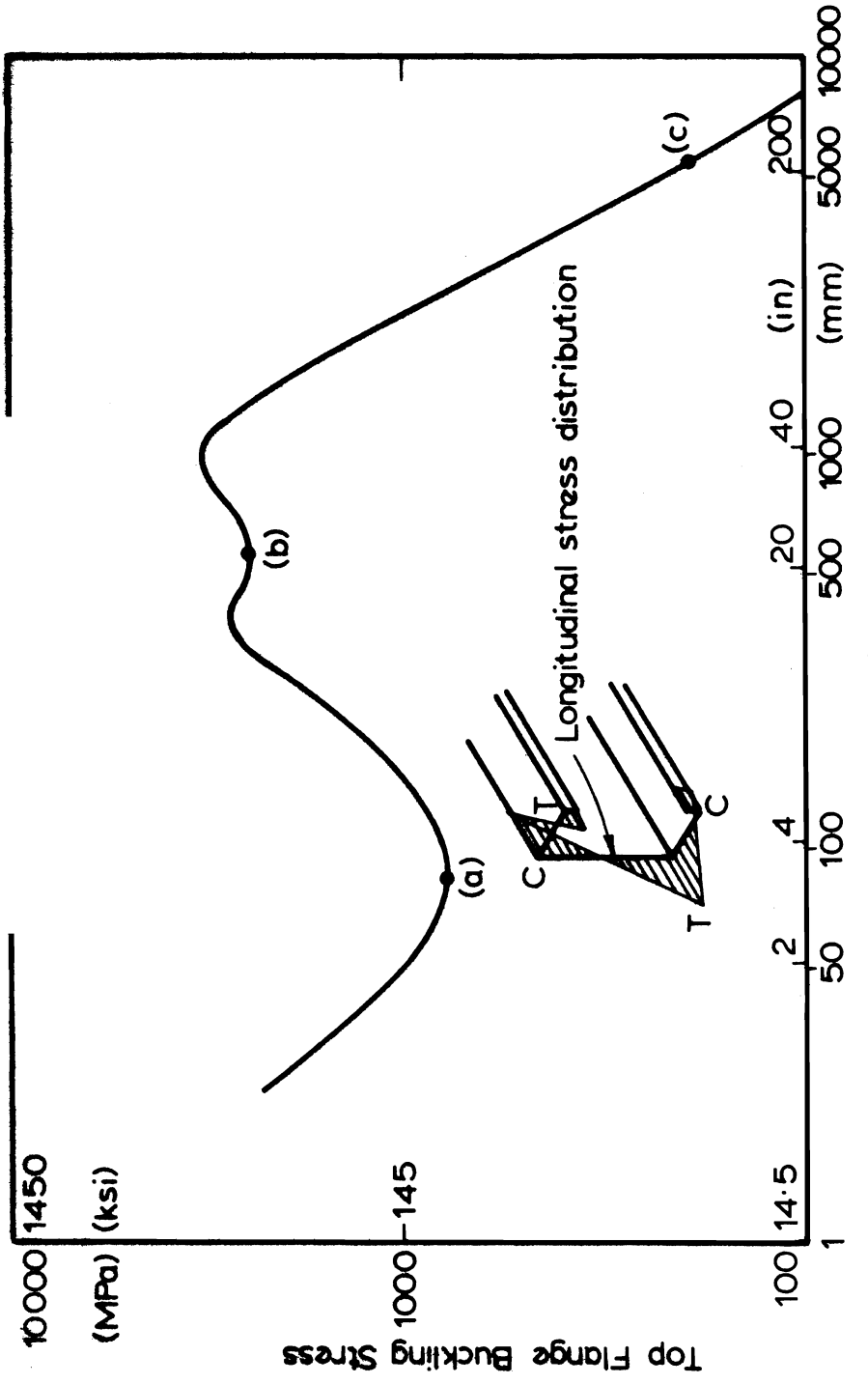

FIG. 10 BUCKLING CURVE FOR CHANNEL SECTION

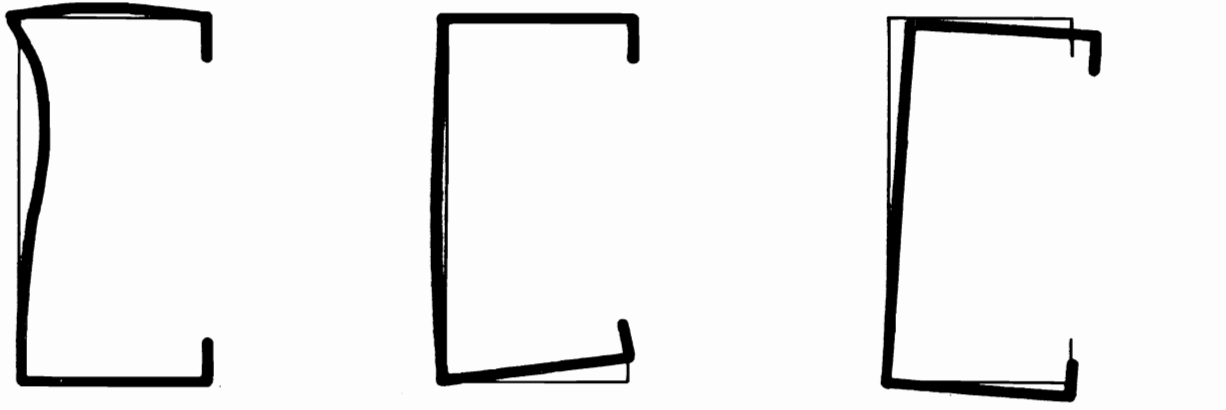

FIG. 11 BUCKLING MODES OF CHANNEL SECTION

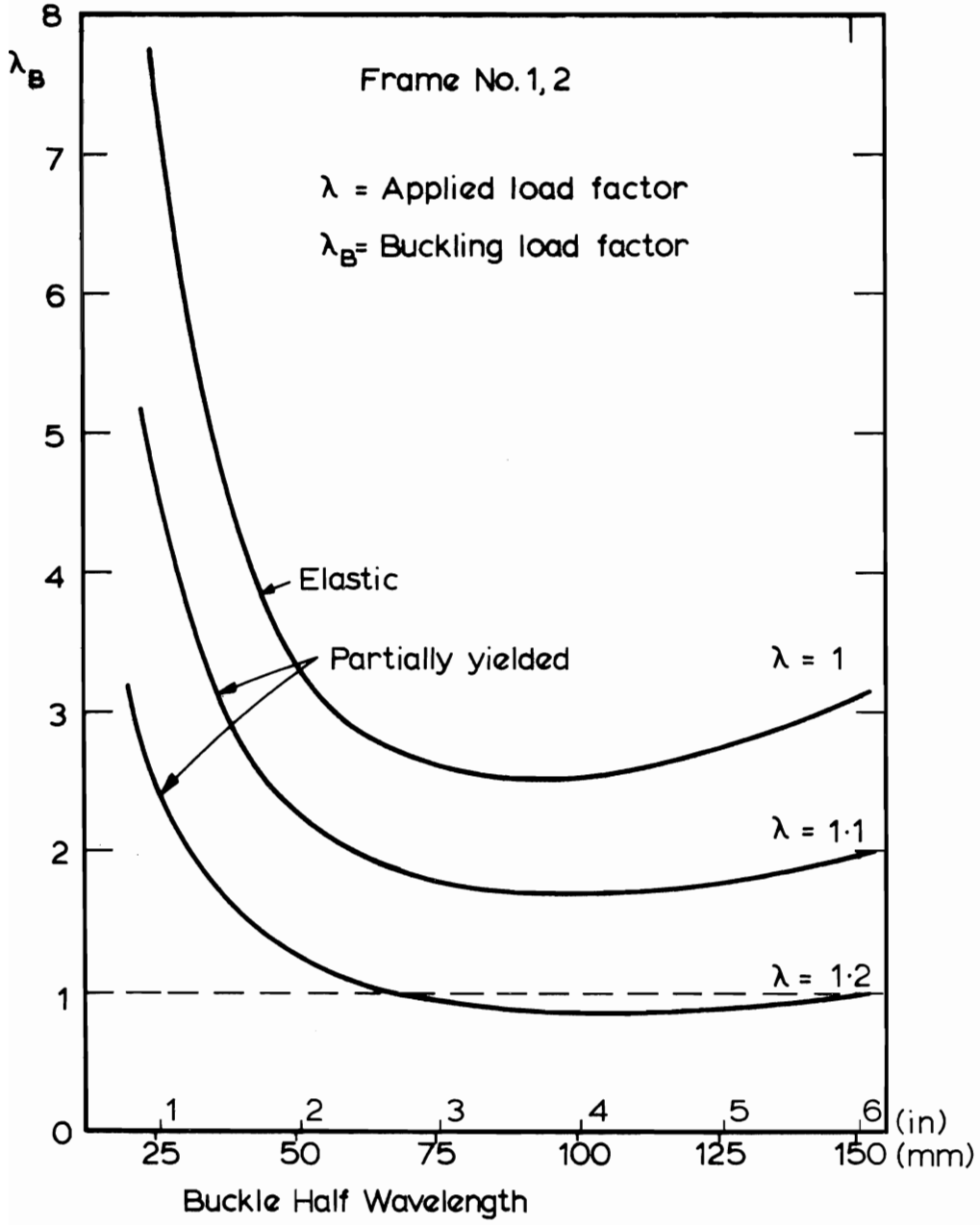

FIG. 12 LOCAL BUCKLING CURVES FOR TOP OF STANCHION —FRAMES 1,2.